

# Thermal heat reservoirs via Gauss' principle of least constraint; Dissipation, chaos, and phase-space dimensionality loss in one-dimensional chains

William G. Hoover  
University of California, Livermore, California 94550

Harald A. Posch  
University of Vienna, Vienna A-1090, Austria

Luke W. Campbell  
University of California, Livermore, California 94550

(Received 8 October 1992; accepted for publication 20 May 1993)

We use Gauss' principle of least constraint to impose different kinetic temperatures on the two halves of a periodic one-dimensional chain. The thermodynamic result is heat flow, as predicted by the Second Law of Thermodynamics. The statistical-mechanical result can be either a phase-space limit cycle or a strange attractor, depending on the chain length and the size of the temperature difference. We document the sensitivity of the Lyapunov spectrum and the underlying phase-space topology by varying the chain length and the size of the kinetic-temperature difference.

## I. INTRODUCTION

Heat, temperature, and entropy are *thermal* variables. They distinguish thermodynamics from mechanics. Because mechanical simulations which incorporate thermal constraints are becoming increasingly important to understanding nonequilibrium flows,<sup>1</sup> we are simulating simple thermomechanical flows, making use of Gauss' and Nosé-Hoover mechanics<sup>2-4</sup> to incorporate kinetic temperature into the equations of motion. The resulting mechanical simulations have all the crucial thermodynamic and hydrodynamic attributes of real macroscopic experiments: nonlinearity, fluctuations, and the irreversible conversion of work to heat. These new mechanics, all with time-reversible deterministic equations of motion, generate both equilibrium and nonequilibrium ensembles analogous to Gibbs' ensembles. For instance, Nosé<sup>3</sup> has shown that the steady state achieved with single-temperature Nosé-Hoover mechanics reproduces Gibbs' canonical ensemble.

Thermal problems require an operational definition of temperature. We adopt the ideal-gas-thermometer definition,  $kT \equiv \langle p^2/m \rangle$  for Cartesian degrees of freedom. This definition has the advantage that the temperature so defined could be measured in a "thought experiment," by exposing the system of interest to elastic impulsive collisions with the atoms making up an equilibrium ideal gas enclosed by a semipermeable membrane.<sup>5</sup>

There are (many) alternative possibilities for defining temperature.<sup>6-8</sup> There are also many ways to impose temperature on selected degrees of freedom, even as a function of location and time. Several deterministic methods, based on differential or integral feedback, can be used to thermostat the kinetic temperature of selected degrees of freedom. These methods simplify theoretical analysis. Unlike stochastic approaches to thermostating, deterministic methods also provide reproducible trajectories, an aid to collaborative work. The simplest thermostating methods, using

feedback, include the *Gaussian* thermostat (based on Gauss' principle of least constraint), which prescribes the kinetic energy, as well as the *Nosé-Hoover* thermostat, which introduces a new temperature control variable into the equations of motion, and the family of *Bulgac-Kusnezov-Bauer* thermostats which typically use *several* control variables in order to guarantee a canonical distribution for otherwise nonmixing systems. These latter forces are sufficient to cause even an otherwise free particle to display classical three-dimensional Brownian motion.<sup>4</sup>

Here we use Gaussian thermostat forces, primarily for simplicity: we wish to adhere as closely as is possible to traditional classical mechanics. Accordingly, temperature enters as a nonholonomic kinetic-energy constraint imposed on an otherwise purely classical motion. Surprisingly, we find that even the simplest possible one-dimensional system, with purely *harmonic*, nearest-neighbor Hooke's law springs, can play the role of a *nonlinear*, dissipative, heat reservoir. It is only required that the kinetic temperature be constrained. We use the Gaussian constraint forces to keep the kinetic energies of two selected groups of degrees of freedom constant in time.

Nonequilibrium systems maintained in stationary states *require* heat exchange with their surroundings, dissipating and depleting external energy sources. The steady-state phase-space distribution corresponding to such a nonequilibrium flow typically occupies either a one-dimensional limit cycle, a few-dimensional torus, or a many-dimensional zero-volume multifractal strange attractor.<sup>9</sup> Very recently Chernov *et al.* have established this multifractal property rigorously for a simple one-body model of electrical conduction.<sup>10</sup> Numerical work, on a variety of systems with as many as 100 atoms, strongly suggests that this multifractal behavior is the generic result of time-reversible simulations of nonequilibrium stationary states. Of course the *projection* of a many-dimensional multifractal distribution onto a few-dimensional subspace can

destroy the fractal character. Accurate *one-body* distributions for gas-phase steady states, such as those obtained from Boltzmann's equation, are continuous.

Fractal phase-space attractors are troublesome for statistical mechanics in many ways. Their singular nature is a telltale symptom of the chaos which underlies them, and which frustrates analytic attempts to describe the distribution. Lacking a smooth distribution, there is no reasonable way to generate a nonequilibrium entropy from a fractal attractor.

*Entropy* has been a traditional means to introduce thermal variables into descriptions of nonequilibrium systems.<sup>11</sup> The fractal nature of our nonequilibrium distributions precludes its use here. Zubarev<sup>12</sup> elaborates a different dynamical approach, much more closely akin to molecular dynamics and related to mesoscopic fluctuation and mode-coupling theories.<sup>6</sup> Our own methods are purely dynamic, and make no explicit use of ensembles. But the dynamical approach we use here is not at all in opposition to traditional ensemble theory. For linear transport, the entropic, Zubarev, fluctuation, and nonequilibrium molecular dynamics approaches all provide results equivalent to Green-Kubo linear-response theory.<sup>2,6,11</sup>

Nonlinear statistical mechanics is still in the early stages of development, and lacks a robust theoretical apparatus for the analysis of far-from-equilibrium chaotic states. We hope that the investigation of simple examples will stimulate advances in broader areas than statistical mechanics. Feedback and thermal reservoirs are as necessary to the modeling and understanding of complex atmospheric and biological systems as they are to purely mechanical systems. To us, the dynamic approach is most basic. This is hardly a new view. In fact, as was emphasized to us by an anonymous referee, the most fundamental of Gibbs' statistical ensembles, the microcanonical ensemble, has its basis in Liouville's theorem. That ensemble uniquely fills the requirement that the dynamic phase-space distribution be stationary. The multifractal nonequilibrium distributions which we find in the present work arise as a consequence of dynamical processes obeying a generalized Liouville's theorem, in which comoving phase-space volumes have an overall tendency to shrink, eventually collapsing onto a strange attractor.<sup>13</sup>

The "Lagrangian" (moving-with-the-flow) smooth contraction and expansion of flows can be described by a phase-space continuity equation while the "Eulerian" (fixed-in-space) distribution *cannot* be so analyzed<sup>13</sup> because the stationary probability density is singular and discontinuous on all scales, no matter how small. Nevertheless, a stationary measure exists.<sup>9,10</sup> The multifractal strange attractors *are singular*, occupying a measure-zero portion of phase-space volume in such a way that the limiting density of points measured in the phase space diverges locally.

It has been amply demonstrated that external fields and moving boundaries can provide chaos, mixing, and dissipation, even in relatively simple few-body systems.<sup>2,11</sup> These simulations typically involve relatively steep anharmonic forces. In this paper, we explore the degree of com-

plexity required for dissipative thermodynamic behavior and we describe the structure of the resulting phase-space distribution functions. Here we approach complexity and dissipation from the simplest possible viewpoint, lattice dynamics, by analyzing a periodic harmonic chain subject to thermal constraints.

Purely harmonic systems lack the "mixing" necessary to satisfy Fourier's linear law, with a heat flux proportional to the temperature gradient. Nevertheless, these systems do satisfy the more general Second Law of Thermodynamics, by transferring heat from hot to cold, and also show phase-space distributions which share the fractal characteristics of more realistic systems. It is because harmonic systems are relatively easy to analyze, and have a long history in statistical mechanics,<sup>14</sup> that we hope that our work stimulates further investigation of these systems. Unlike the earlier work, which generally relies on an infinite number of "bath" degrees of freedom, our own work, as well as that of Ref. 4, suggests that as few as three or four degrees of freedom can represent a heat reservoir.

We consider an  $N$ -particle one-dimensional chain, with cyclic ("periodic") boundary conditions, and subject to *nonholonomic* (velocity-dependent) constraints which maintain a nonequilibrium steady state. The corresponding (cubic) anharmonic constraint forces introduce coupling among the chain modes and make the dynamics "interesting" and dissipative.

Nonequilibrium systems maintained in stationary states require heat exchange with their surroundings, dissipating and depleting external energy sources. Such a steady heat exchange lies outside Hamiltonian mechanics. Thermal energy can *only* be extracted by velocity-dependent forces. The traditional method for non-Hamiltonian heat transfer has been the Langevin equation. Heat has been extracted with a phenomenological viscous drag force and introduced with a stochastic force. Time-reversible alternatives have the advantage of portability and reproducibility as well as easing the analysis. Here we choose Gaussian constraint forces to maintain the temperature of selected sets of degrees of freedom.

Our Gaussian thermal constraints fix the temperatures in two  $(N/2)$ -mass sections of the chain. The two sections correspond to cold and hot "reservoirs." For simplicity, the reservoir temperatures are kept constant, and the particles at the same temperature are contiguous. For simplicity, we also fix the centers of mass of the two "reservoir" regions. For convenience, we choose the particle masses, equilibrium spacing, and nearest-neighbor spring constants all equal to unity.

Among the many ways that thermal constraints can be implemented, Gauss' principle of least constraint is the simplest. Though it is ordinarily reliable, the principle is *not foolproof*.<sup>2,15</sup> It works by selecting the *smallest possible* constraint forces according to Gauss' variational principle:

$$\delta \sum \frac{F_c^2}{(2m)} \equiv 0.$$

Here, and in what follows, the sums indicated by  $\Sigma$  are to be taken over *all* appropriate constrained degrees of freedom. To enforce the four constraints,

$$\left\{ \Sigma \left( \frac{p_T^2}{m} \right) \equiv 2K_T; \Sigma p_T \equiv 0 \right\}; T \equiv \text{COLD or HOT},$$

straightforward application of the principle<sup>2</sup> provides four Lagrange multipliers,  $\{\zeta_{\text{COLD}}, \zeta_{\text{HOT}}, \eta_{\text{COLD}}, \eta_{\text{HOT}}\}$ :

$$\left\{ \zeta_T \equiv \frac{\Sigma(Fp/m)_T}{\Sigma(p^2/m)_T}; \eta_T \equiv \frac{\Sigma F}{\Sigma 1} \right\}.$$

These multipliers appear in the equations of motion:

$$\left\{ \frac{dq}{dt} \equiv p; \frac{dp}{dt} \equiv F + F_C \equiv F - \zeta_T p - \eta_T \right\},$$

where  $F_C$  is Gauss' constraint force,  $-\zeta_{\text{COLD}}p - \eta_{\text{COLD}}$  for cold particles and  $-\zeta_{\text{HOT}}p - \eta_{\text{HOT}}$  for hot ones. The constraints of reservoir momentum, imposed by  $\eta_{\text{COLD}}$  and  $\eta_{\text{HOT}}$ , have an additional consequence for the coordinates: the centers of mass of the two thermostated regions,  $\{(2/N)\Sigma q\}$ , are constants of the motion. Thus the four momentum constraints actually correspond to six phase-space constraints, and reduce the dimensionality of the accessible phase space from  $2N$  to  $2N-6$ .

Simultaneous constraints of vanishing total momentum and fixed kinetic energy  $K$  have only one solution for two atoms, and that solution is not useful. The two momenta are  $\pm [2mK]^{1/2}$ , so that the two coordinates diverge to  $\pm \infty$  linearly in time. Thus, at least *three* atoms are required in any thermal reservoir. In the simplest case ( $N=6$ ), with three "cold" particles and three "hot" ones, the momenta are restricted to two ellipses:

$$\begin{aligned} p_3 &\equiv -p_1 - p_2 \Rightarrow [p_1^2 + p_2^2 + p_3^2]/2 \\ &\equiv p_1^2 + p_1 p_2 + p_2^2 \equiv (3/2)mkT_{\text{COLD}}; \end{aligned}$$

$$\begin{aligned} p_6 &\equiv -p_4 - p_5 \Rightarrow [p_4^2 + p_5^2 + p_6^2]/2 \\ &\equiv p_4^2 + p_4 p_5 + p_5^2 \equiv (3/2)mkT_{\text{HOT}}. \end{aligned}$$

Specifying two momenta, one cold and one hot, and four coordinates, two cold and two hot, is enough for a six-dimensional phase-space description. Thus a subspace  $\{q_1, p_2, q_3, q_4, p_5, q_6\}$  is sufficient to describe the thermally driven motion of six particles. In this representation the remaining variables,  $\{p_1, q_2, p_3, p_4, q_5, p_6\}$ , can all be obtained from the constraint equations. We refer to this approach as "Method  $2N-6$ ."

An alternative to this reduced description is to impose the constraints while solving for the motion in the *full* phase space,  $\{q_1, q_2, q_3, q_4, q_5, q_6, p_1, p_2, p_3, p_4, p_5, p_6\}$  in the example just discussed. We refer to this approach as "Method  $2N$ ." From the *mathematical* standpoint, the Lagrange multipliers included in the equations should constrain the motion to a  $2N-6$  dimensional subspace. But, in every case the equations turn out to be Lyapunov unstable (so that initially insignificant *computational* errors, in the last decimal place, grow large *exponentially fast*). For this reason, it is necessary to insist on double-precision accu-

racy in the integration, and to remove the small drifts in kinetic energy and center-of-mass location from time to time. If this is not done, the numerical results can diverge.

The instability of *chaotic* flows is conveniently described through the Lyapunov spectrum  $\{\lambda\}$ , where we adopt the conventional ordering:  $\lambda_1 \geq \lambda_2 \geq \lambda_3 \dots$ . The Lyapunov spectrum is the collection of the orthogonal *comoving* exponential divergence (and convergence) rates in the appropriate phase space. By definition, the time-averaged rate at which *two* nearby trajectories diverge is  $\exp(\lambda_1 t)$ . The comoving area with vertices defined by *three* such phase-space trajectories diverges (or collapses) as  $\exp(\lambda_1 t + \lambda_2 t)$ , and so on.

To diagnose the complete phase-space topology of the motion there are two straightforward possibilities. In Method  $2N$  we follow the progress of a set of  $2N$  infinitesimal orthonormal offset vectors<sup>16</sup>  $\{\delta_1, \delta_2, \dots, \delta_{2N}\}$  which span a moving  $2N$ -dimensional hypersphere in the  $2N$ -dimensional space. The hypersphere is centered on a moving reference system. The comoving space spanned by the offset vectors can be called "tangent space" if the length of the offset vectors is infinitesimal, rather than just small. The  $2N$  offset vectors can be visualized as linking the main "reference" trajectory to  $2N$  nearby "satellite" trajectories. The relative motion of the satellite trajectories is often linearized, corresponding to choosing infinitesimal lengths for the offset vectors. Because each of the vectors has  $2N$  components, all told  $2N(2N+1)$  coupled equations need to be solved when this approach is followed. In the present paper we have used Benettin's method<sup>17</sup> to extract the Lyapunov spectrum from the motion of the satellite trajectories. We warn the reader that Method  $2N$ , unless followed with due care, can lead to errors and misrepresentations in problems with constraints, as is outlined below.

Method  $2N-6$  is more nearly foolproof, and follows the motion of just  $2N-6$  independent offset vectors in the  $(2N-6)$ -dimensional tangent subspace which corresponds to fixed values of all six constrained sums,  $\{\Sigma q_T, \Sigma p_T, \Sigma(p_T^2/m)\}_{T=\text{COLD or HOT}}$ . The nonlinearity of the kinetic-energy constraints makes this approach slightly more difficult to program. One might well (erroneously) expect (as we did at first) that the nonzero Lyapunov exponents would be identical for the two choices,  $2N$ -dimensional space or  $(2N-6)$ -dimensional space. Instead, the two methods of analysis give quite different results, with the unconstrained-space spectrum seriously wrong. Nevertheless, there is an interesting correspondence between Method  $2N$  and Method  $2N-6$ . *All*  $2N-6$  correct Lyapunov exponents are present in either case. But the naive version of Method  $2N$  introduces six new artificial exponents (which can be positive or negative). The presence of these extra nonvanishing spurious exponents was, for us, surprising. It complicates the analysis of phase-space topology in the presence of nonlinear constraints.

## II. ANALYSIS AND RESULTS

We mentioned that the momentum constraints require a minimum of three particles in each reservoir. Accordingly we investigated the two simplest cases possible, six-

particle and eight-particle chains. The six-particle case corresponds to a six-dimensional constrained dynamics with five-dimensional Poincaré sections which can be analyzed graphically. Three of the five dimensions can be used to locate  $\{x,y,z\}$  Cartesian coordinates with the other two used to orient  $\{\theta,\phi\}$  a vector based at  $(x,y,z)$ .

We verified that sufficiently long (millions of time steps) double-precision simulations with sufficiently small time steps (0.005, with masses, energies, and vibrational frequencies of order unity) produce reproducible averages, with statistical uncertainties independent of the time step. Our first simulations used the naive (false) version of Method  $2N$ . These results invariably included at least one positive Lyapunov exponent, suggesting the presence of a multifractal strange attractor.

Our attempts to corroborate this assumed multifractal-strange-attractor interpretation soon revealed a difficulty. Despite positive Lyapunov exponents, all the six-particle trajectories which we examined in detail approached robust limit cycles! More investigation revealed the cause of this paradox: the positive six-particle exponents were actually *false*, a spurious consequence of computer round-off error coupled with unphysical instabilities lying outside our constraint surfaces. Here is a brief explanation:

Consider a six-particle *reference trajectory*, in 12-dimensional phase space, but restricted to a six-dimensional subspace defined by the constrained values of the six sums  $\{\Sigma q_T, \Sigma p_T, \Sigma(p_T^2/m)\}_{T=\text{COLD or HOT}}$ . Consider as well a second six-particle *satellite trajectory*, and use Benettin's distance-rescaling technique to keep this satellite trajectory close to the first. In 12-dimensional space distance means  $[\Sigma\{\Delta q^2 + \Delta p^2\}]^{1/2}$ . If both trajectories are followed in the full six-particle 12-dimensional phase space, but *with the separation between the reference and satellite trajectories constrained*, by rescaling, and with the six constraints  $\{\Sigma q_T = \text{const}, \Sigma p_T = 0, \Sigma(p_T^2/m) = 2K_T\}$  imposed at every time step (so that neither the reference nor the satellite trajectory can drift away from the six-dimensional constraint subspace) *there is no measurable positive Lyapunov exponent*. Thus the largest Lyapunov exponent is zero for the six-particle chains and the motion occupies either a one-dimensional limit cycle or a few-dimensional torus.

On the other hand, if the satellite trajectory is not separately forced (by removing the effects of computer rounding errors) to follow the nonlinear kinetic-energy constraints, *rotation* of the reference-to-satellite vector off the constraint surface gives a positive Lyapunov exponent, the signature of chaos. Rotation causes an unconstrained satellite trajectory to weave back and forth through the constraint surface  $\{p_1^2 + p_2^2 + p_3^2 \equiv 3mkT_{\text{COLD}}; p_4^2 + p_5^2 + p_6^2 \equiv 3mkT_{\text{HOT}}\}$ . The unphysical "instability" which then results gives rise to a false positive Lyapunov exponent. In fact, when properly constrained, the satellite trajectories all occupy periodic orbits with no positive Lyapunov exponents.

The *eight-particle* chains can behave in a very different, more complex, way, though they also can exhibit (false) dimensionality reductions if the dynamics is not properly

constrained. The effect of the nonlinear constraints can be demonstrated by following two eight-particle constrained trajectories, restricting both to the constrained  $16-6=10$ -dimensional subspace. When the resulting motion is found to be Lyapunov unstable (exponentially growing separation between the two trajectories), the maximum Lyapunov exponent turns out to be considerably less than that found by the "naive" unconstrained reference-satellite technique. As a specific example, consider an eight-particle chain with cold and hot kinetic energies of 0.3 and 1.7, respectively (the atomic mass, equilibrium spacing, and Hooke's law force constant are all taken to be unity). The maximum Lyapunov exponent found using the naive version of Method  $2N$  in the full 16-dimensional Cartesian phase space is 0.19. If the separation in the constrained ten-dimensional space is considered instead (by constraining the cold and hot satellite kinetic energies) the maximum Lyapunov exponent is three times smaller, 0.063.

To aid those readers who wish to repeat these calculations, or to pursue others ones using Gaussian mechanics, we outline the simplest numerical method for imposing the appropriate constraints on the tangent vectors for the correct version of Method  $2N$ , using the eight-particle case to illustrate.

It is convenient to impose all six constraints together, at regular intervals of a few time steps. After computing (fourth-order Runge-Kutta integration is the most convenient choice) the ten ( $2N$  less six constraints) new offset vectors:

$$\{\delta\} = \{\delta q_1, \delta q_2, \delta q_3, \delta q_4, \delta q_5, \delta q_6, \delta q_7, \delta q_8, \\ \delta p_1, \delta p_2, \delta p_3, \delta p_4, \delta p_5, \delta p_6, \delta p_7, \delta p_8\},$$

the center-of-mass constraints can be imposed by subtracting mean values. For instance each of the offset vectors has the four coordinate offsets of the "cold" particles  $\{1,2,3,4\}$  reduced by  $(\delta q_1 + \delta q_2 + \delta q_3 + \delta q_4)/4$  and the momentum offsets reduced by  $(\delta p_1 + \delta p_2 + \delta p_3 + \delta p_4)/4$ . The kinetic energy constraints imply additionally that both the cold and hot sums,

$$\{p_1\delta p_1 + p_2\delta p_2 + p_3\delta p_3 + p_4\delta p_4 \text{ and } p_5\delta p_5 + p_6\delta p_6 + p_7\delta p_7 \\ + p_8\delta p_8\},$$

vanish. Lagrange-multiplier analysis then shows that each of the cold and hot momentum offsets,  $\{\delta p_i\}$  and  $\{\delta p_j\}$ , respectively, should be reduced by

$$\frac{\Sigma(p\delta p/m)_{\text{COLD}}p_i}{\Sigma(p^2/m)_{\text{COLD}}} \text{ or } \frac{\Sigma(p\delta p/m)_{\text{HOT}}p_j}{\Sigma(p^2/m)_{\text{HOT}}}.$$

It is satisfying to verify that these adjustments make negligible differences in the local (time varying) Lyapunov exponents, but do serve to constrain the global trajectories of the offset vectors to the portion of tangent space satisfying all six constraints.

In the more direct Method  $2N-6$  the motion of the  $2N-6$  tangent vectors is followed by integrating sets of linearized motion equations. Including the reference trajectory this means that a total of  $(2N-6)(2N-5)$  first-order

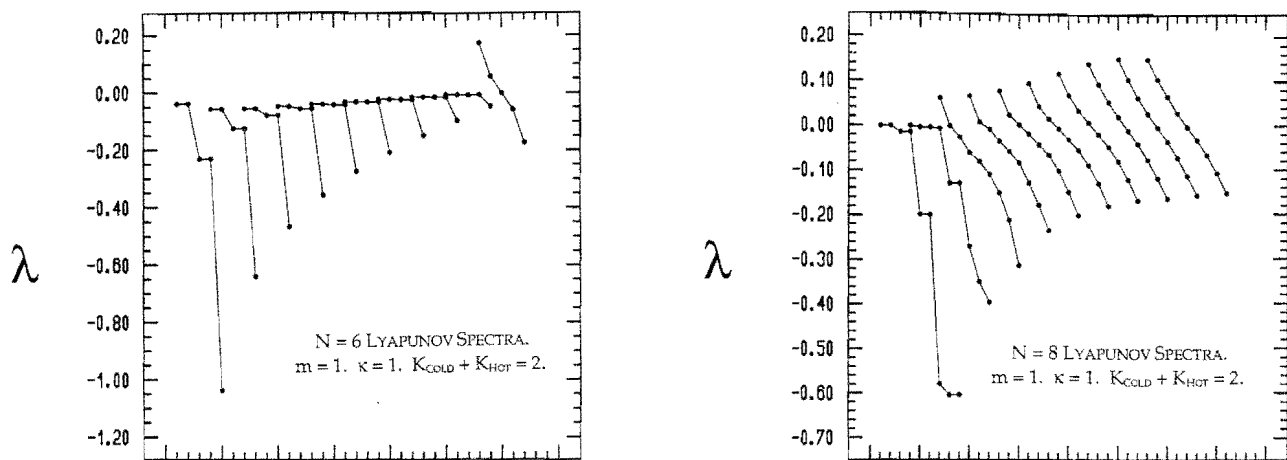


FIG. 1. Lyapunov spectra for periodic chains of six (left) and eight (right) particles are shown as dots connected by lines. There is a separate curve for each of the ten cases shown in Table I. The temperature difference between the cold and hot reservoirs increases from zero (at the right) to the maximum of 1.9–0.1 (at the left). The equilibrium spectrum corresponding to the equal-kinetic-energies case is at the right. The six center-of-mass and kinetic energy constraints have been taken into account here and the vanishing exponent associated with motion along the constrained phase-space trajectory has also been suppressed, so that a total of  $2N-7$  exponents are shown. For six particles, except in the equilibrium case, all five exponents are negative, and correspond to a stable limit cycle. For eight particles, except very far from equilibrium, at least one of the nine exponents is positive, corresponding to a chaotic multifractal strange attractor.

ordinary differential equations need to be solved. For eight particles the reduced phase-space state could be specified by the set

$$\{q_1, q_2, q_3, q_5, q_6, q_7, p_1, p_2, p_5, p_6\},$$

with the remaining set,  $\{q_4, q_8, p_3, p_4, p_7, p_8\}$ , determined from the constraints. The tangent vectors would likewise have components

$$\{\delta q_1, \delta q_2, \delta q_3, \delta q_5, \delta q_6, \delta q_7, \delta p_1, \delta p_2, \delta p_5, \delta p_6\}.$$

The remaining set,  $\{\delta q_4, \delta q_8, \delta p_3, \delta p_4, \delta p_7, \delta p_8\}$ , could be recovered from the derivatives of the corresponding constraints:

$$\left\{ \sum \delta q_T = 0, \sum \delta p_T = 0, \sum \left( \frac{p \delta p}{m} \right)_T = 0 \right\};$$

$T = \text{COLD or HOT.}$

We eliminated programming and algorithmic errors by diligently testing and cross-checking a variety of methods. Both the correct version of Method  $2N$  and Method  $2N-6$  gave identical results. Independent calculations were carried out in Livermore and Vienna.

The Lyapunov spectra found for both the six- and the eight-particle chains are displayed in Fig. 1. In the figure we show the  $2N-7$  exponents remaining after imposing the six phase-space constraints on center of mass and kinetic energy, and after eliminating the zero exponent corresponding to motion along the trajectory direction. For both the six- and eight-particle chains the largest of the Lyapunov exponents,  $\lambda_1(6)$  and  $\lambda_1(8)$ , are given in Table I. Except in the equilibrium situation the six-particle chain has no positive exponents.

Two-dimensional phase-plane plots  $\{q, p\}$  of the individual particles' trajectories are the best means we have

found for portraying the eight-particle trajectories. In Fig. 2 we show, for the eight-particle chain, the variation of single-particle orbits for four different values of the cold and hot temperatures. For small temperature differences the motion is delocalized and chaotic. For very large temperature differences the motion approaches a limit cycle. For moderate temperature ratios a positive Lyapunov exponent results. Fluctuations in the exponent indicate that the motion occupies a multifractal strange attractor. For the highest temperature differences (always with the total cold+hot kinetic energy fixed) the eight-particle strange attractor achieves a one-dimensional limit cycle. An example appears in the upper left-hand corner of Fig. 2.

To suggest the way in which these short-chain results approach the large-chain limit, we show in addition, in

TABLE I. Dimensional contraction  $\Delta D$ , external dissipation rate  $dS/dt$ , and largest Lyapunov exponent  $\lambda$  as functions of temperature difference in six-atom (6) and eight-atom (8) one-dimensional harmonic chains. The offset vectors linking satellite trajectories to a constrained reference trajectory were restricted to six- and ten-dimensional subspaces of tangent space. The total kinetic energy is 2 in all cases. These data were obtained from the last half of simulations carried out with either 200 000 000 (six particles) or 100 000 000 (eight particles) time steps of length  $dt=0.001$ .

$K_C$	$K_H$	$\Delta D(6)$	$\Delta D(8)$	$\dot{S}/k(6)$	$\dot{S}/k(8)$	$\lambda_1(6)$	$\lambda_1(8)$
1.0	1.0	0.0	0.0	0.0	0.0	0.174	0.152
0.9	1.1	5.0	0.15	0.22	0.04 <sub>6</sub>	0.00	0.152
0.8	1.2	5.0	0.5 <sub>8</sub>	0.45	0.18	0.00	0.14
0.7	1.3	5.0	1.2 <sub>2</sub>	0.70	0.39	0.00	0.118
0.6	1.4	5.0	2.1 <sub>7</sub>	0.97	0.64	0.00	0.096
0.5	1.5	5.0	3.2 <sub>5</sub>	1.29	0.92	0.00	0.078
0.4	1.6	5.0	4.3 <sub>4</sub>	1.67	1.27	0.00	0.067
0.3	1.7	5.0	5.3	2.20	1.76	0.00	0.063
0.2	1.8	5.0	8.0	3.01	2.56	0.00	0.000
0.1	1.9	5.0	9.0	4.72	4.43	0.00	0.000

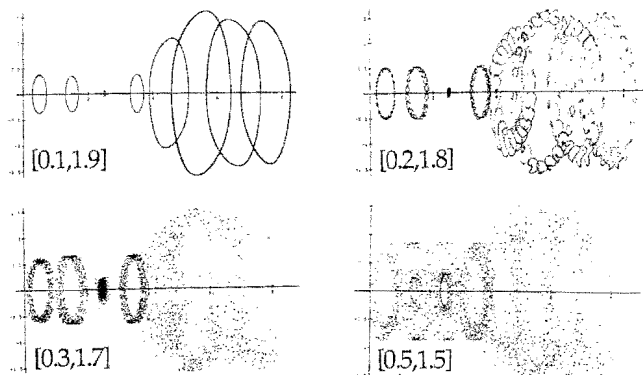


FIG. 2. Single-trajectory phase-plane plots (momentum is the ordinate and coordinate the abscissa) for eight-particle chains after the initial decay of transients. Kinetic energies of the cold and hot regions are indicated. The pair [0.1, 1.9] is a limit cycle. The plotting interval for the pair [0.2, 1.8] was specially chosen to emphasize the nearly periodic nature of the nonchaotic orbit.

Figs. 3 and 4, the analogous phase-plane plot for a 64-particle chain together with its complete Lyapunov spectrum (127 exponents). For the temperature difference shown, with  $T_{\text{COLD}}/T_{\text{HOT}}=0.1/1.9$ , the motion displays no positive Lyapunov exponents so that the motion occupies a few-dimensional torus. We have made no attempt to carry out a comprehensive analysis of many-particle chains. It would be interesting to analyze the way in which these chains approach a continuum limit described by partial differential equations. In the idealized case of chains obeying Fourier's law (which our own chains do not) and with a temperature-independent heat conductivity, the steady temperature profile would have to satisfy the coupled pair of diffusion equations:

$$\nabla^2 T_{\text{COLD}} \propto +T_{\text{COLD}}; \quad \nabla^2 T_{\text{HOT}} \propto -T_{\text{HOT}}.$$

Our own computer-generated temperature profiles have a

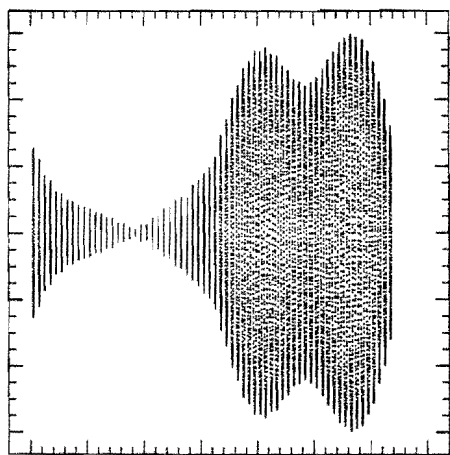


FIG. 3. Single-trajectory phase-plane plots (momentum is the ordinate and coordinate the abscissa) for a 64-particle chain with cold and hot kinetic energies of 0.1 and 1.9, respectively.

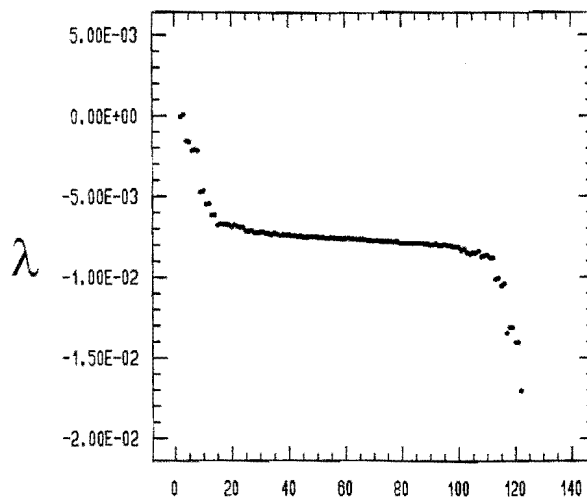


FIG. 4. Lyapunov spectrum (127 exponents, with a single zero suppressed) for the 64-particle chain corresponding to the trajectory shown in Fig. 3. The last half of a simulation with a total time of 20 000 was used to generate these data.

more complicated structure than does this Fourier law diffusion-equation solution (a hyperbolic cosine in the cold region and a cosine in the hot one).

The data in Table I show (see the columns giving  $\dot{S}/k$ ) a nearly linear increase in flow with temperature differences in the six-atom chain, but a more nearly quadratic variation in the eight-atom chain. The large-system profile shown in Fig. 3 does show a temperature minimum in the middle of the cold region, but has *three* definite extrema in the hot region. These smooth profiles together with the relatively simple mathematical structure of the underlying harmonic chain suggest that a continuum analysis of these profiles and of the relation between overall heat flux and temperature difference might be possible. We have made no progress in that direction.

Kaplan and Yorke<sup>18</sup> pointed out that a phase-space object with a Lyapunov exponent sum of zero neither grows nor shrinks (exponentially) with time. Thus the information dimension of a phase-space attractor, with  $\sum \lambda < 0$ , can be estimated by counting the number of Lyapunov exponents required for the partial sum  $\sum' \lambda$ , starting with the largest exponent and adding successively more negative ones, to vanish,  $\sum' \lambda \equiv 0$ . The "Kaplan-Yorke dimension" uses linear interpolation in calculating the non-integral dimension interpolated between successive exponent sums.<sup>18</sup> We have calculated this dimension using the Lyapunov spectra from Fig. 1.

As we mentioned, Kaplan-Yorke dimensions, calculated with *unconstrained* satellite dynamics, are simply incorrect, and suggest strange attractors for systems which may actually follow limit cycles or inhabit few-dimensional tori. The *correct* (constrained) Kaplan-Yorke dimensions, for a variety of cold-to-hot temperature ratios, appear in Table I. In phase-space dimensionality  $\Delta D$  is the *loss*, and  $\Delta D$  is necessarily bounded between 0 (the equilibrium value) and the maximum occupied dimensionality less one,

$2N-7$ . This largest possible reduction corresponds to a phase-space limit cycle.

With either Gaussian or Nosé-Hoover thermostats there are simple relations linking the Lyapunov exponents  $\{\lambda\}$ , the contraction rate of phase-space hypervolume, the external entropy production  $dS/dt$ , and the friction coefficients  $\{\xi\}$ . Such relations can be derived from Liouville's theorem<sup>2,8</sup> by considering the flow of probability density  $f(\{q,p\}_N)$  in the full  $2N$ -dimensional phase space, taking into account the constraints which restrict the flow to a  $(2N-6)$ -dimensional subspace. Despite the fractal nature of the underlying phase-space distribution, the theorem can be correctly applied to the analysis of phase-space flows in a comoving (as opposed to fixed) frame.<sup>13</sup>

The Lagrange multipliers  $\eta_{\text{COLD}}$  and  $\eta_{\text{HOT}}$  do not influence the "comoving" time derivatives of the phase-space volume,  $\otimes$ , or the probability density,  $f$ , where both derivatives are measured in a coordinate system moving with the flow. The Lagrange multipliers  $\xi_{\text{COLD}}$  and  $\xi_{\text{HOT}}$  lead to the contraction and expansion, respectively, of the comoving phase volume  $\otimes$ . In the *constrained* phase space (correctly taking the four momentum constraints into account) the following relations hold:

$$\begin{aligned} -\sum' \lambda &\equiv \left\langle \frac{-d \ln \otimes'}{dt} \right\rangle \equiv \left\langle \frac{d \ln f'}{dt} \right\rangle \\ &\equiv \left\langle \sum' \left[ \xi + p \left( \frac{\partial \xi}{\partial p} \right) \right] \right\rangle \\ &\equiv \frac{(N-4)}{2} \langle [\xi_{\text{COLD}} + \xi_{\text{HOT}}] \rangle \\ &\equiv \frac{[(N-4)/(2N)] d(S/k)}{dt} \end{aligned}$$

Here the primes indicate the restriction to a  $(2N-6)$ -dimensional subspace of the phase space within which the six constraints are satisfied. We have verified all of these several connections numerically. They provided useful checks on the programming of the motion equations for the offset vectors.

### III. DISCUSSION

Our results show that the simplest possible thermostat, a Gaussian constraint force on the kinetic energy, provides an adequate thermal bath for a purely harmonic one-dimensional system. Aside from the two nonholonomic constraints, the dynamics is conventional Newtonian dynamics. Because the underlying system is harmonic, the very interesting features our simulations reveal suggest the system as a fertile ground for theoretical analysis. These same reservoirs might also prove useful in constructing mechanical models of biological systems.

For us, the major surprise in this work was the intricate topological character of the phase-space distributions. The six-particle nonequilibrium problems all converge to limit cycles or tori, though a standard method of analysis, the naive Method  $2N$ , would wrongly suggest higher-dimensional strange attractors. The eight-particle results

show up the difficulty even better. The Lyapunov exponents themselves depend strongly upon whether or not constraints are explicitly imposed on the satellite trajectories. Unconstrained satellite trajectories appear to be considerably less stable (larger maximum Lyapunov exponents) than satellite trajectories with constrained kinetic energies. The present work shows that the nonlinear nature of the thermal constraint can change the magnitude of the Lyapunov exponent by as much as a factor of 3. We also find that nonlinear constraints present in a reference system need to be explicitly incorporated in satellite systems too, to avoid tangent-space rotational forces.

Another crucial feature of these calculations, obvious in retrospect, but frustrating prior to discovery, was the need for brute-force implementation of the center-of-mass constraints, both in coordinates and momenta, to avoid drift. This sensitivity would have been more difficult to uncover in a typical three-dimensional many-body simulation.

Intuition suggests that the loss of phase-space dimension  $\Delta D$  should behave quadratically for small deviations from equilibrium. The results shown in Table I are consistent with this idea. The first few small-deviation eight-particle data suggest the relationship,

$$\begin{aligned} (\Delta D)/(D-1) &\approx 1.7 [(K_{\text{HOT}} - K_{\text{COLD}})/ \\ &\quad (K_{\text{HOT}} + K_{\text{COLD}})]^2. \end{aligned}$$

Here,  $D$  is the total embedding dimension of the constrained phase space, 10, so that, for the maximum temperature difference, the eight-particle  $\Delta D$  must be 9, corresponding to a limit cycle. This small-deviation parabola for  $\Delta D$  turns out also to be nicely consistent with a vanishing maximum Lyapunov exponent, corresponding to a limit cycle, for  $K_{\text{HOT}}$  greater than 1.75. This threshold value for chaos agrees with that found numerically (by carrying out nine simulations equally spaced in kinetic energy, with  $K_{\text{HOT}}$  between 1.70 and 1.80) within the numerical uncertainty of 0.01.

The fact that substantial losses in dimensionality occur in an otherwise purely Newtonian system, subject only to thermal nonholonomic constraints, strongly suggests, as we found previously,<sup>19</sup> that similar dimensionality reductions could be found in simulating two- or three-dimensional systems. Larger-scale simulations can be better carried out when computer capacities have increased.<sup>20</sup>

### ACKNOWLEDGMENTS

At Livermore this work was performed under the auspices of the U.S. Department of Energy at the Lawrence Livermore National Laboratory, pursuant to Contract No. W-7405-Eng-48. Computations at the University of Vienna were supported by the University Computer Center, operating within the framework of the IBM European Academic Supercomputer Initiative, and by the Austrian Fonds zur Förderung der Wissenschaftlichen Forschung,

Grant No. P8003. Luke Campbell was supported by University of California Faculty Research Grant No. 3-521002-19900 from the University of California at Davis. We thank David Boercker, Jeff Kallman, Joel Keizer, Doug Miller, and Steve Volkman (supported by the Academy of Applied Science), for providing inspiration, and advice. The three referees provided several helpful clarifying suggestions.

<sup>1</sup>G. Ciccotti, D. Frenkel, and I. R. McDonald (editors), *Simulation of Liquids and Solids* (North-Holland, Amsterdam, 1987); *Microscopic Simulations of Complex Flows*, edited by M. Mareschal (Plenum, New York, 1990).

<sup>2</sup>For general background, consult W. G. Hoover, *Computational Statistical Mechanics* (Elsevier, Amsterdam, 1991).

<sup>3</sup>S. Nosé, *J. Chem. Phys.* **81**, 511 (1984).

<sup>4</sup>D. Kusnezov, A. Bulgac, and W. Bauer, *Ann. Phys.* **204**, 155 (1990); **214**, 180 (1992); D. Kusnezov, *Phys. Lett. A* **166**, 315 (1992).

<sup>5</sup>W. G. Hoover, "Nonequilibrium Molecular Dynamics," in the conference proceedings on *Dynamical Fluctuations and Correlations in Nuclear Collisions* (Aussois, France, 16–20 March 1992), edited by E. Saraud, *Nucl. Phys. A* **545**, 523c (1992).

<sup>6</sup>For an overview, see J. Keizer, *Statistical Thermodynamics of Nonequilibrium Processes* (Springer-Verlag, Berlin, 1987).

<sup>7</sup>L. S. Garcia-Colin and M. S. Green, *Phys. Rev.* **150**, 153 (1966).

<sup>8</sup>D. Jou and J. Casas-Vázquez, *Phys. Rev. A* **45**, 8371 (1992).

<sup>9</sup>B. L. Holian, W. G. Hoover, and H. A. Posch, *Phys. Rev. Lett.* **59**, 10

(1987); H. A. Posch and W. A. Hoover, "Nonequilibrium Molecular Dynamics of Classical Fluids," in the Proceedings of the NATO Advanced Science Institute at Luso, Portugal: *Molecular Liquids: New Perspectives in Physics and Chemistry*, edited by J. J. C. Teixeira-Dias, (Kluwer, Dordrecht, The Netherlands, 1992).

<sup>10</sup>N. I. Chernov, G. L. Eyink, J. L. Lebowitz, and Ya. G. Sinai, *Phys. Rev. Lett.* **70**, 2209 (1993); note also the related paper, W. N. Vance, *Phys. Rev. Lett.* **69**, 1356 (1992).

<sup>11</sup>D. J. Evans and G. P. Morriss, *Nonequilibrium Liquids* (Academic, New York, 1990).

<sup>12</sup>D. N. Zubarev, *Nonequilibrium Statistical Thermodynamics* (Consultants Bureau, New York, 1974).

<sup>13</sup>See, for instance, B. L. Holian, G. Ciccotti, W. G. Hoover, B. Moran, and H. A. Posch, *Phys. Rev. A* **39**, 5414 (1989); B. L. Holian, H. A. Posch, and W. G. Hoover, *ibid.* **42**, 3196 (1990).

<sup>14</sup>H. Spohn and J. L. Lebowitz, *Commun. Math. Phys.* **54**, 97 (1977).

<sup>15</sup>W. G. Hoover, B. Moran, and J. M. Haile, *J. Stat. Phys.* **37**, 109 (1984).

<sup>16</sup>H. A. Posch, W. G. Hoover, and B. L. Holian, *Ber. Bunsen-Gesellschaft Phys. Chem.* **94**, 250 (1990).

<sup>17</sup>G. Benettin, L. Galgani, and J.-M. Strelcyn, *Phys. Rev. A* **14**, 2338 (1976).

<sup>18</sup>J. Kaplan and J. Yorke, "Chaotic behaviour of multidimensional difference equations," in *Functional Differential Equations and the Approximation of Fixed Points*, Lecture Notes in Mathematics, edited by H. O. Peitgen and H. O. Walthier (Springer-Verlag, Berlin, 1980), Vol. 730.

<sup>19</sup>W. G. Hoover, H. A. Posch, and C. G. Hoover, *Chaos* **2**, 245 (1992).

<sup>20</sup>R. Preston, "The Mountains of Pi," *The New Yorker*, 2 March, 36 (1992).